Rheology modification in mixed shape colloidal dispersions. Part II: mixtures†

Annemieke J. W. ten Brinke,[a] Louise Bailey,[b] Henk N. W. Lekkerkerker[a] and Geoffrey C. Maitland*[c]

Received 29th August 2007, Accepted 9th November 2007
First published as an Advance Article on the web 29th November 2007
DOI: 10.1039/b713144e

We report the results of a comprehensive study of the rheological properties of a series of mixed colloid systems where the shape of one of the components has been varied systematically. Specifically we have measured the oscillatory, transient (creep) and continuous steady shear flow behaviour of a 2.5 wt% dispersion in water of a well-characterised hectorite clay modified by the addition of a series of aluminasol colloidal particles whose shape varies systematically from rod (boehmite) to platelet (gibbsite) to sphere (alumina-coated silica), all having essentially the same smallest dimension, which is similar to that of the hectorite. The particle characterisation and rheological properties of the pure components have recently been reported in Part I of this series (*Soft Matter*, 2007, **3**, 1145). The mixtures show the same general behaviour as the pure systems, displaying a complex 'yield space' transition from an elastoviscous gel at low applied stresses to a viscous, weakly elastic, shear-thinning liquid at high stresses. The unifying theme of this work is that the addition of 0.25 wt% of the minor component in all cases results in dramatic enhancements to the dispersion rheological properties. At the same time the magnitude of this effect depends on the shape of the particles. Shear moduli, low stress viscosities and effective yield stresses all increase in the additive order rods < platelets < spheres, with enhancements for the latter being up to a factor of 500 and typically 20. At the same time the critical failure strains for the gels decreased in the same order – the strongest gels are also the most fragile in this sense. The physicochemical factors underlying this behaviour are discussed and a simple qualitative model described. While no complete explanation or model can be proposed at this stage, the study provides a quantitative model-system baseline for mixed colloidal dispersions already used for industrial applications (*e.g.* oilwell-drilling fluids) and suggests ways in which such fluids may be optimised and controlled.

Introduction

Non-spherical colloidal dispersions are used in a wide range of industrial applications that exploit their unique elasto-plastic rheological behaviour. For example, colloidal clay particles find application in oilfield- and construction-drilling fluids.[2–4] In low ionic strength environments these highly anisotropic particles gel at relatively low suspension volume fractions ~1–4%, due to overlap of their large effective hydrodynamic volumes, demonstrating high low-shear viscosities and a high effective 'yield stress'. Once this 'yield stress' is overcome the suspensions are strongly shear-thinning. On cessation of flow the suspension re-gels on timescales of the order of seconds to tens of minutes. These properties enable the clay suspension to suspend the large dense particles of the drilling cuttings and weighting agent (~μm–mm) at rest, and require relatively low pump power during circulation.

The properties of suspensions of highly anisometric colloids, such as rods[5,6] and platelets,[7] have been widely studied, in particular the industrially important clays kaolin[8], laponite,[9] and montmorillonite.[10,11] While particles of extreme anisotropy may show a rich liquid-crystalline phase diagram,[12] in general one observes a gel phase that arrests crystallisation.[13] In the semi-dilute regime they form a stiff repulsive gel. Shear induces alignment of the particles, thereby reducing overlaps and apparent viscosity. On cessation of shear, flow is quenched and the particles randomly orient. Over time, through cooperative Brownian motion of the particles, the suspension rebuilds structure. It can be seen that the rheological properties, which reflect the suspension microstructure, are highly dependent on the shear history and the pathway to the gel state. As discussed in Part I of this series,[1] variations in these shear- and time-dependent properties can arise from quite subtle differences in the fundamental characteristics of the particles: the size, shape, flexibility, surface charge (sign, spatial distribution and density).

The rheological and thixotropic properties of suspensions can be enhanced through the addition of a small fraction, typically < 10% of the clay content, of a second colloidal component. In the drilling-fluids domain, the addition of magnesium aluminium hydroxide ($Mg_{2-x}Al_x(OH)^{x+}_2$ or MMH) colloid to a montmorillonite suspension in the ratio

[a]*Van't Hoff Laboratory for Physical and Colloid Chemistry, Utrecht University, Padualaan 8, 3584 CH Utrecht, the Netherlands*
[b]*Schlumberger Cambridge Research, High Cross, Madingley Road, Cambridge, UK CB3 OEL*
[c]*Department of Chemical Engineering, Imperial College London, South Kensington, London, UK SW7 2AZ*
† Electronic supplementary information (ESI) available: Kelvin model parameters and creep analysis. See DOI: 10.1039/b713144e

1 : 10 results in the very rapid ($\sim$10 s) formation of a strong gel immediately after cessation of flow.[2] On application of a shearing flow, the gel structure breaks down rapidly, resulting in highly shear-thinning behaviour and $\eta(\dot{\gamma} \rightarrow \infty)$ values close to that of water ($\dot{\gamma}$ = shear rate). The MMH particles are hexagonal plates, much smaller and less flexible than montmorillonite (diameter $\sim$100 nm, aspect ratio $\sim$ 10) and are positively charged in contrast to the negatively charged montmorillonite at pH $>$ 8. The strong coulombic attractions between the two colloid types, along with the rapid Brownian rotational and translational diffusion of the smaller MMH, combine to give the rapid structural rearrangements on start-up and cessation of flow reflected in the yield stress dynamics.[3,4] The fluid viscosity increases and the gelation recovery time after shearing is reduced from minutes to seconds. This heterocoagulation of montmorillonite with MMH and related hydrotalcite materials has been studied[14] over the mass fraction, χ, range $0.2 < \chi < 0.94$; maxima of the yield stress and the storage modulus have been found for $0.4 < \chi < 0.5$. It has also been shown that MMH–hectorite[15] and MMH–attapulgite[4] mixtures also demonstrate desirable rheological properties, with subtle differences as the clay component is changed, although most of the MMH studies have used industrial precipitates of ill-defined shape. One major disadvantage of these MMH-extended fluids is that the presence of significant salt levels, often present in drilling fluids used for offshore applications or in drilling through saline formations, screens the key attractive electrostatic interactions between the platelets leading to a loss of rapid gelation and fall in viscosity/shear modulus. This renders them incapable of suspending solid particles or maintaining laminar flow, for example. This sensitivity implies that the origin of the rheology enhancement is primarily due to attractive electrostatic bridging interactions between the oppositely charge platelets. Recently, other colloidal minerals, gibbsite ($Al(OH_3)$) and boehmite (AlO(OH)), have also been shown to act as montmorillonite extenders.[16] These mixed suspensions give similar rapid gelation on cessation of flow and high shear-thinning on start-up but are found to be far less sensitive to salt and to temperature than montorillonite–MMH mixtures. The questions surrounding the origins of such effects are in part why these systems merit further study. One purpose of the present study is to explore them in detail and to demonstrate that they are generic characteristics of many mixed colloid systems.

Using model colloids much better characterised than these commercial systems, researchers have begun to study how addition of a second colloidal component of different size, shape or charge affects the properties of a suspension, particularly the phase behaviour. Lekkerkerker and co-workers[17,18] have demonstrated that the phase behaviour of mixed platelet–rod-sphere systems is extremely rich. The kinetics and arrest of crystallisation, phase separation and appearance of amorphous, glass-like sediments in such mixed systems have also been studied.[19] Lewis and Rhodes,[20] Louis *et al.*[21] and others have shown that small colloidal particles can give rise to both attractive and repulsive depletion interactions between larger colloids, depending on their relative size and charge. Baird and Walz[22,23] have recently published studies on the effect of spherical silica nanoparticles on the gelation of plate-like kaolin suspensions. Yet the rheological properties and the underpinning particle-scale dynamics of mixed size-shape colloid systems have been relatively little studied.

Here we present the first systematic study of the effect of particle shape on the rheological enhancement in colloid systems caused by addition of a small amount of a second component, using well-characterised colloidal particles. To gain insight into the dynamic behaviour of mixed colloid dispersions, we have studied suspensions of model particles with a systematic variation in anisotropy (length L_1, width L_2 and thickness d) from a lath-like hectorite clay ($L_1 > L_2 > d$), to rod-like boehmite ($L_1 > L_2 \sim d$), and plate-like gibbsite ($L_1 \sim L_2 > d$) aluminasols. In Part I[1] we presented results of a systematic multi-technique rheological study (oscillatory, transient and steady shear) carried out on these model systems. These systems demonstrated a rich rheological behaviour that could be rationalised in terms of flow-mediated building and disruption of microstructure. At very low strain the system behaved as an elastoviscous solid with a very high viscosity, at high strain/strain rates as a shear-thinning low viscosity liquid. The transition between the two is complex and cannot be defined by a single parameter such as the yield stress; instead there is a 'yield space', which requires a range of parameters and timescales to describe it and which is a function of both the current structural state of the material and its stress–strain-time history. Strain appears to be the critical parameter for initial gel failure.

In this second paper we investigate the rheological behaviour of mixtures of these colloids, and how addition of a small amount of the second component can dramatically alter the rheological properties of the suspension. We believe that this is the first systematic attempt to map out this behaviour using well-characterised model colloidal systems. We consider the mixtures lath + rod, lath + plate, and to complete the systematic variation in particle shape, lath + sphere using cationic alumina-coated silica spheres (Ludox CL). We make use of the systematic multi-technique rheometric approach that we developed in Part I, which allows us to characterise the full rheological behaviour from elastoplastic solid to viscous liquid.

Experimental

Materials: preparation and characterisation

Hectorite, SHCa-1, was supplied by the Clay Minerals Society, Source Clay Repository, and the $>$2 μm fraction was separated by sedimentation. Gibbsite and boehmite were synthesised in-house following the techniques of Van Bruggen[24] and Wierenga *et al.*[7] The colloids were dialysed against demineralised water for 14 days. Ludox Silica AS40 (anionic) and CL (cationic, alumina-coated silica) supplied by Sigma-Aldrich were used as supplied. Table 1 reprises the characterisation of the colloids detailed in paper I.

As in Part I we have compared the different colloid dispersions at essentially the same total mass concentrations in order to emphasise the effects of particle size and shape on the gelation properties. Industrial applications seek maximum exploitable effect (here the extent and rate of forming or destroying a gel) for minimum material loading/cost. To

Table 1 Particle characteristics of the model colloids studied in this work

	Particle			
Property	Hectorite	Gibbsite	Boehmite	Ludox CL[e]
Shape	Lath	Plate	Rod	Sphere
L_1/nm	288	81	200	12
L_2/nm	43	81	10	12
d/nm	6	6[a]	10	12
Density/g cm^{-3}	2.39	1.96	2.06	2.2
α[b]	160	6.8	200	
C^*/g per 100 cm^3[d]	1.5	28.8	1.1	
pH[c]	8.9	7.8	6.2	4.5
Sign of face charge	−	+	+	+
Conductivity/μS cm^{-1}	38.1 @ 1336 ppm	80.2 @ 1154 ppm	46.0 @ 1045 ppm	
Mobility/10^{-8}m^2 Vs^{-1}	−1.2	2.8	3.9	
Zeta potential/mV	−9.8	+24.0	+44.2	+42

[a] Determined from AFM, the other d values are estimated from TEM. [b] Ratio of hydrodynamic volume V_h ($4\pi(L_1/2)^3/3$) to real particle volume ($\sim L_1L_2d$) [c] Natural pH of suspensions after dialysis. [d] C^* is the 'overlap concentration' at which the hydrodynamic volumes swept out by the particle's largest dimension start to overlap = $(100L_1L_2 \times 24d\rho)/4\pi L_1^3$. [e] Literature data.

prepare the mixtures 2.5 wt% suspensions of hectorite and the second component were mixed in a ratio of 10 (hectorite) to 1 (aluminasol), giving a hectorite–aluminasol weight ratio of 0.091 : 0.909. The mixtures were stirred vigorously with a mechanical stirrer and used without adjustment of native pH or added electrolyte.

Rheological measurements

Steady shear, creep and oscillatory experiments were carried out on the mixtures using a Physica Anton Paar (MCR-300) controlled stress rheometer, with a smooth cone-plate geometry with a diameter of 5 cm and a cone angle of 1°. All measurements were carried out at 20 °C. A second set of measurements were made using a Bohlin CVO rheometer with a micro-roughened cone-plate geometry having a diameter of 4 cm and a cone angle of 4°. The same measurement protocols were adopted in each case and extremely good agreement between measurements on similar samples was obtained, increasing our confidence in the phenomena observed.

All the suspensions show thixotropic behaviour, reflecting the finite time taken to move from any one state of microstructure to another as a result of the competition between break-down of the interacting colloidal network due to flow stresses and its build-up due to flow-induced collisions and Brownian motion. Consequently, to ensure reproducibility it was necessary to use a well-defined sample loading and pre-treatment protocol to ensure that the measurements were independent of sample history and to wait for the shear stress to come to a steady-state value at each imposed shear rate.[25] In Part I two such pre-treatment protocols were adopted for steady shear measurements: a) broken gel, 60 s pre-shear at a shear rate of 500 s^{-1}; b) equilibrium gel, 60 s pre-shear at a shear rate of 500 s^{-1} followed by 1000 s recovery at rest. It was found that the results obtained for the two pre-treatments were essentially identical; consequently only the results for the equilibrium gel protocol will be presented here.

Two different types of oscillatory shear experiments were carried out to measure the storage (G') and loss modulus (G'') components of the frequency (ω)-dependent complex shear modulus $G^*(\omega) = G'(\omega) + iG''(\omega)$ (see Goodwin and Hughes[26]). At low strains (γ), or deformation amplitudes, these parameters are constant (the so-called linear viscoelastic regime) whereas at higher strains they decrease and their viscoelasticity becomes non-linear. To investigate this in amplitude sweep experiments, the measuring time at each value for the strain amplitude was 22 s (4 s equilibration, followed by 18 s measurement time) and the frequency was set at 1 Hz. To investigate the frequency dependence (frequency sweep experiments) an optimum measuring time was selected for each frequency (increasing with decreasing frequency) and a constant strain amplitude of 0.05 (chosen to operate as far as possible within the linear viscoelastic regime) was applied. The frequency sweep was executed from high to low frequency in order to maximize the effect of the pre-treatment and therewith improve the reproducibility of the measurements. Total run times are of the order of 4 hours, consequently the low frequency points are determined when the sample has been gelling for a considerable time.

Time constants characteristic of the network dynamics can be determined from creep measurements. Here a stress, τ_0, was applied to the sample and the strain response γ was recorded as a function of time. After the stress had been applied for a time, t_1, chosen to ensure that the creep response had reached a steady state ($d\gamma/dt = 0$ or a constant), it was removed, and recovery of the strain $\gamma(t)$ was recorded. For these experiments the equilibrium gel pre-treatment protocol was used with a shorter rest recovery period of 200 s. These data were used to define a time-dependent creep modulus $J(t) = \gamma(t)/\tau_0$, or its inverse, a creep modulus $G(t)$. In the limit of zero time, the instantaneous values of these quantities $G(t \rightarrow 0)$, $G_e = 1/J_e$ are equivalent to the infinite frequency values of G', commonly called the plateau modulus.

For the continuous steady shear experiments, stress–strain and stress–strain rate flow curves were obtained both for controlled stress and controlled strain rate conditions. The measuring time at each imposed strain rate or shear stress, determined from separate experiments to be adequate for achieving steady-state, was 54 s (24 s equilibration time, followed by 30 s measurement time). Part I showed that for the pure components, the stress–strain rate curve is non-monotonic and consequently different parts of it are revealed in the two types of experiment. At each point on the curve, an effective viscosity $\eta(\dot{\gamma})$ can be defined as $\tau/\dot{\gamma}$.

Results

Hectorite–boehmite

This mixture of lath and rod-like particles was studied in similar detail to the pure components as described in Part I,[1] with the full range of rheological experiments detailed above. Fig. 1 shows the storage and loss moduli (G', G'') as a function of strain amplitude at 1 Hz for the hectorite–boehmite mixture compared to the pure hectorite suspension. The behaviour of the mixture is qualitatively similar to the pure hectorite suspension,[1] with a high-modulus gel at low strains,

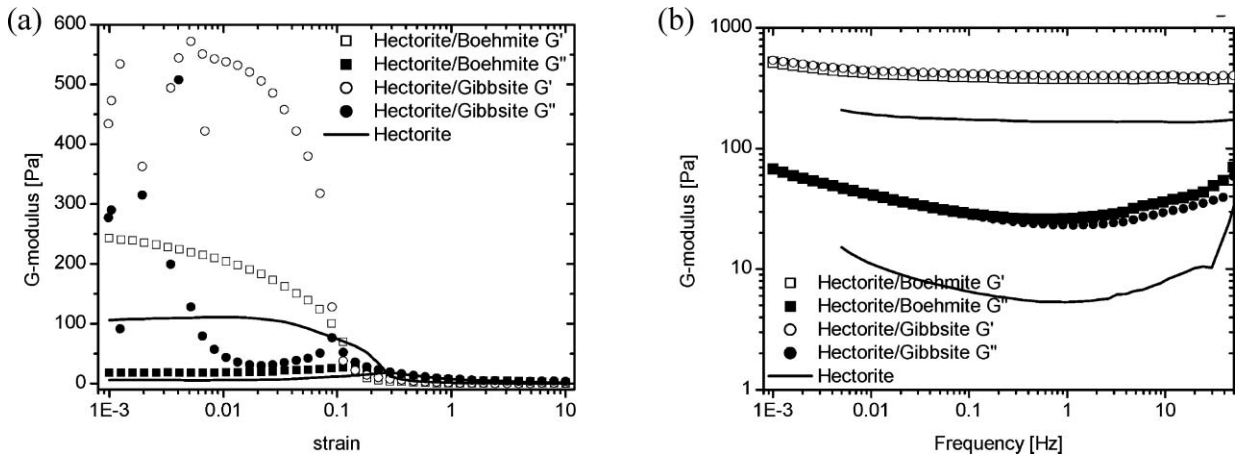

Fig. 1 (a) Amplitude sweep, and (b) frequency sweep for mixtures of hectorite–boehmite and hectorite–gibbsite as compared to a suspension of pure hectorite at the same (solids) concentration. The data for pure hectorite represented by the solid lines are taken from ref 1.

transforming to a low modulus liquid at high strains, the transition defined by two critical strains, the initial critical strain, γ_c, where G' first becomes non-linear and a yield strain, γ_y, where the storage and loss moduli curves cross. As with the pure minerals, the pre-treatment protocol has little effect on the yield behaviour with about a 20 Pa difference in G' between the equilibrium and broken gel reflecting the 100 s longer gelation time.

However, adding just 0.25 wt% of boehmite rods results in some marked quantitative differences. Hectorite shows a distinct plateau in G' before starting to yield at a strain of $\sim$0.01, whereas the mixture already shows some yield at γ = 0.001, and a gradual drop through γ = 0.01 similar that seen with the pure boehmite suspension, although with no inflection point. The major drop in G' occurs between γ_c = 0.01–0.1 and the crossing of the G', G'' curves occurs at $\gamma_y \sim 0.15$, significantly lower than in the single component suspensions ($\gamma_y \sim$ 0.35–0.4). The most dramatic difference is the increase of G' in the linear region for the mixture (250 Pa) compared to the pure components (100 Pa for hectorite and negligible for boehmite at 0.25 wt%; at 1.5 wt% G' is only 30 Pa). It appears that the addition of a small amount of boehmite, with only a minor perturbation on the effective hydrodynamic volume fraction of the suspension, more than doubles the modulus whilst reducing the yield strain by a factor of 2–3.

We now turn to the frequency dependence of the complex shear moduli in the linear regime as shown in Fig. 1b. As seen with the pure components,[1] the curves are again rather structureless, with G' remaining essentially frequency independent and G'' about an order of magnitude lower until it starts to rise slowly above 3 Hz and rapidly above 30 Hz. The gradual rise in both moduli towards lower frequencies demonstrates the developing structure in the suspension as it continues to gel over the extended measurement time.

As we have seen in the amplitude sweeps, the moduli are a factor of 2–3 higher for the mixture than for the single component suspensions. The growth in storage modulus over time (for ω = 0.5 Hz and γ = 0.05), after ceasing steady shear flow is shown in Fig. 2. This shows that in both cases there is a rapid initial gelation, reaching about 70% of its limiting value in <30 s followed by a slower long term approach to final steady value in about 600 s.

Next we examine the yielding behaviour of the mixture in creep experiments, as shown in Fig. 3. The suspensions shows an instantaneous elastic response, characterised by an initial creep compliance $J_e = \gamma_e/\tau$, followed by a time-dependent creep region, leading finally to a linear flow region whose slope gives the (very low) shear rate corresponding to the imposed stress (the strain overshoot seen at small times and small applied stresses is an instrumental artefact arising from the finite inertia of the measurement assembly).

As with the pure components, a simple generalised Kelvin model can be used to describe the creep curves:

$$\gamma(t) = \gamma_e + \sum_i \bar{\gamma}_i \left[1 - e^{\frac{-t}{\lambda_i}}\right] + \frac{t\tau}{\eta(\tau)}$$

where λ_i are retardation times characterising the creep behaviour, τ is the applied stress, $\eta(\tau)$ the effective viscosity = $\tau/\dot{\gamma}$, where the

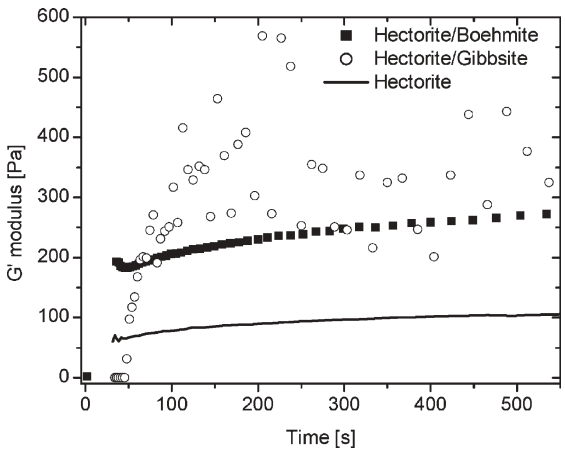

Fig. 2 Growth of storage modulus G' over time for mixtures of hectorite–boehmite and hectorite–gibbsite as compared to a 2.5 wt% suspension of pure hectorite. The data for pure hectorite represented by the solid line are taken from ref 1.

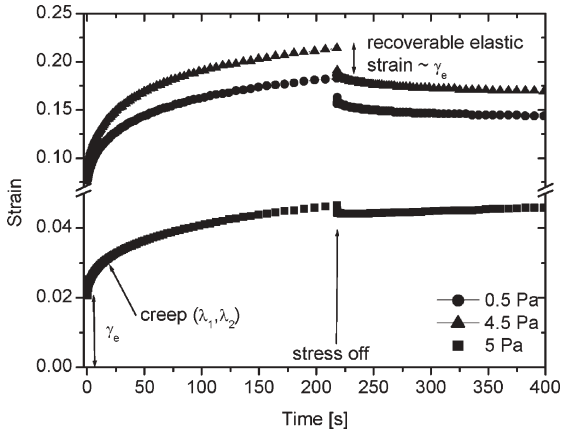

Fig. 3 Creep curves for the hectorite–boehmite mixture at imposed stresses 0.5 Pa, 4.5 Pa and 5 Pa.

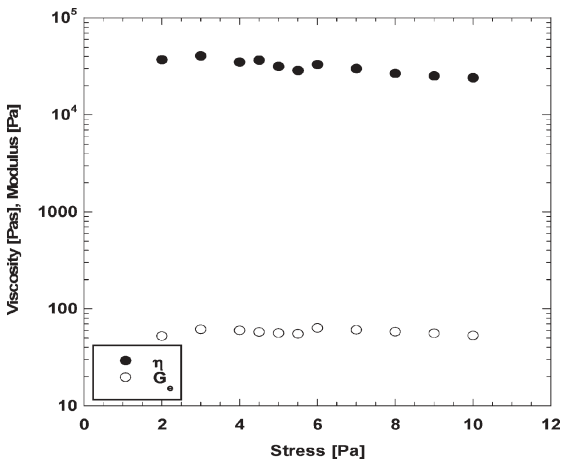

Fig. 4 Creep viscosity $\eta(\tau)$ and plateau modulus G_e as a function of applied stress for the hectorite–boehmite mixture.

shear strain rate $\dot{\gamma}$ is simply the limiting slope of the linear flow region. Two retardation times were found sufficient to describe the creep of these fluids. The parameters for the Kelvin model fit for each applied stress, together with the plateau modulus $G_e = J_e^{-1}$, are given in the ESI†.

The same qualitative behaviour is observed as with pure hectorite.[1] As seen in Fig. 4, G_e has an essentially constant value of 58 $\pm$ 5 Pa, which is in-line with the values from oscillatory measurements at comparable strains. The retardation times are compared to the hectorite values in Fig. 5. There is a peak in both retardation times at $\tau \sim 2$ Pa as in the pure hectorite.[1] Below 2 Pa, the mixture's retardation times are about half those of the pure hectorite and have a lower stress dependence. Above $\tau \sim 2$ Pa, the stress dependence increases and above $\tau \sim 4$ Pa the retardation times are increasingly greater than those of hectorite. This reflects the fact that λ_1 and λ_2 for hectorite decrease rapidly as its effective yield stress of 9 Pa is approached[1] and the system loses its elasticity, whereas the mixture still shows no sign of yielding, and is still significantly elastic, at an applied stress of 10 Pa. This is a dramatic demonstration of the enhanced gel elasticity caused by addition of a small fraction of boehmite rods to the hectorite lath suspension. The prolongation of the pre-yield low stress effective viscosity can be seen in Fig. 4 which shows that $\eta(\tau)$ decreases only slightly from its low-stress value of about 4×10^4 Pa s up to an applied stress of 10 Pa, which is clearly still below its yield region. $\eta(\tau)$ is determined using the slope of the strain–time plot (= strain rate $\dot{\gamma}$) at long times, typically 5–7 long retardation times (λ_1), in order to ensure that no retarded viscoelasticity effects remain.

Now we turn to the flow curves under continuous shear. For controlled-stress continuous shear, we see (Fig. 6a) the same type of complex flow curves as were observed for the single component dispersions,[1] and appears to be characteristic of these systems. On ramping up the stress, the mixture has initially a low shear viscosity of $\sim 10^5$ Pa s, and we see the shear-thickening 'hook' to the flow curve at the lowest shear rates as the system begins to strain and rearrange. At a stress of 22 Pa the system yields, jumping several decades of shear rate to the high shear – low viscosity branch, to a shear rate of ~ 500 s^{-1}. The transition to the high shear branch takes place from a similar shear rate to the pure hectorite suspension, but at a significantly higher stress. If we plot the data in terms of

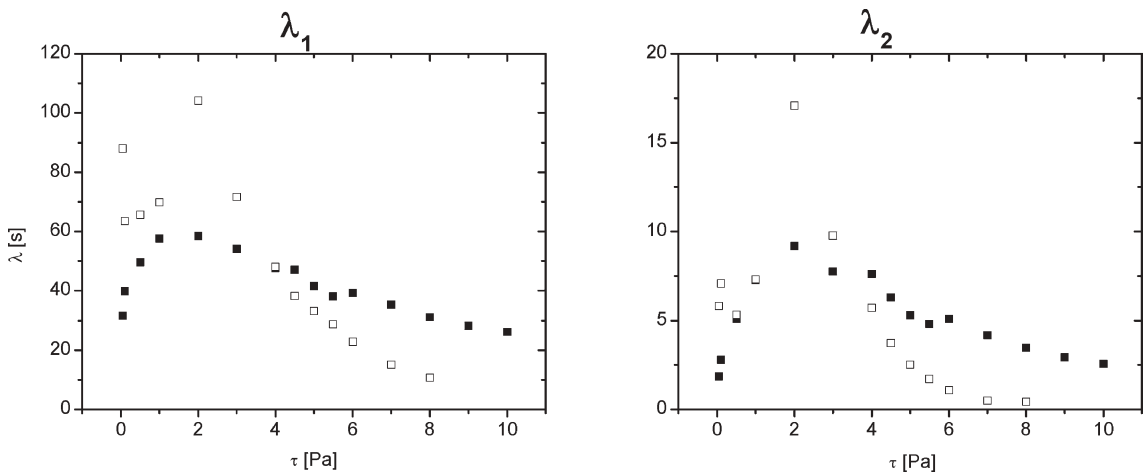

Fig. 5 Retardation times for 2.5 wt.% hectorite (open markers) and for the 2.5/0.2 wt% hectorite–boehmite mixture (filled markers) as a function of applied stress.

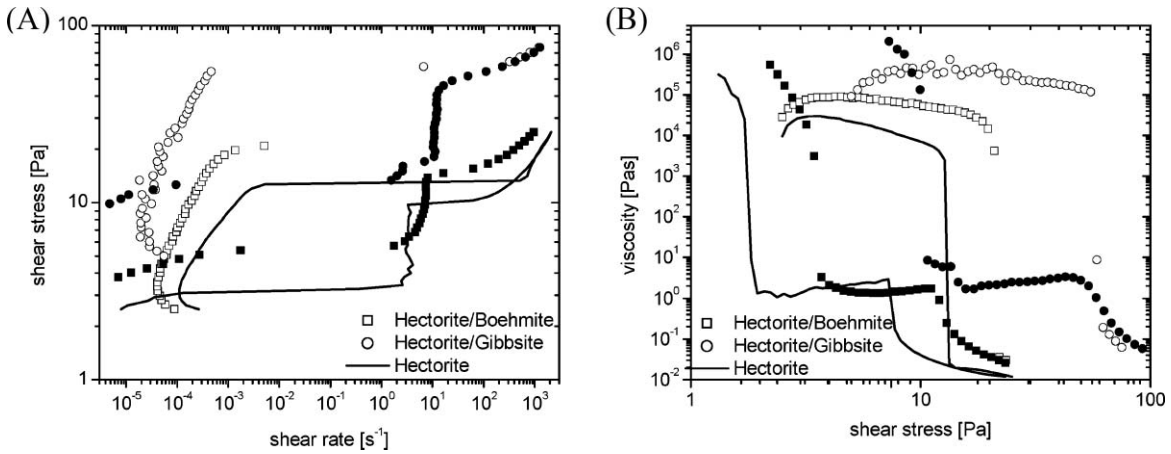

Fig. 6 Flow curves for mixtures of hectorite–boehmite and hectorite–gibbsite for equilibrium gels as compared to pure hectorite: (A) controlled shear stress–shear rate; (B) controlled shear stress–viscosity. Open symbols up-ramp shear stress, closed symbols down-ramp shear stress.

apparent viscosity *vs.* shear stress, Fig. 6b, this behaviour corresponds to the suspensions rapidly shear thinning at an effective yield stress of 22 Pa.

On ramping down the shear stress the fluid follows this low viscosity branch to a stress of 14 Pa, dropping to 5 Pa at a shear rate of around 3 s^{-1} as the suspension moves back onto the low shear–high viscosity branch. The flow curve for the boehmite–hectorite mixture in Fig. 6a is displaced upwards from the pure hectorite suspension, indicative of its enhanced rheology. Fig. 6b shows clearly the low shear viscosity of the mixture has increased from the pure hectorite by about a factor of 3 to 10^5 Pa s and the effective yield stress from 13 to 22 Pa.

Table 2 summarises the rheological parameters for the hectorite–boehmite mixture obtained from the steady shear and transient techniques. Again a picture emerges of a gelling fluid having a plateau modulus $G'_{(\gamma\to 0)}$ of 250 Pa and an effective viscosity of 10^5 Pa s at low stresses, transforming from a elasto-viscous gel to a viscoelastic liquid at a critical 'yield' or transition stress of 22 Pa where it becomes a shear-thinning suspension of high stress viscosity about 10 Pa s and a power law exponent $\sim$0.5. These values are all significantly higher than for the pure hectorite gel whereas the transition strains of $<$0.001 for initial onset and $\sim$0.15 for the yield strain are both lower than for hectorite alone, indicating that the more strain-sensitive boehmite[1] is playing a critical role in the enhancement of the gel structure.

Hectorite–gibbsite

We now examine the mixture of lath-like (hectorite) and plate-like (gibbsite) particles. Fig. 1a shows the storage and loss moduli as a function of strain amplitude at 1 Hz for the hectorite–gibbsite mixture compared to the pure hectorite suspension. The data at low strain are noisy, but it is clear that the enhancement of G' is even more marked than for the hectorite–boehmite mixture. The maximum value at low strains is $\sim$550 Pa; this decreases initially at $\gamma_c \sim 0.01$ and

Table 2 Summary of rheological parameters for hectorite and hectorite–boehmite, hectorite–gibbsite, hectorite–Ludox CL mixtures obtained by a range of techniques

		2.5 wt% hectorite		2.5 wt% hectorite–0.25 wt% boehmite		2.5 wt% hectorite–0.25 wt% gibbsite		2.8% hectorite–0.25% Ludox CL[a]
		BG[d]	EG[d]	BG	EG	BG	EG	EG
Strain amplitude sweep	$G'_{(\gamma\to 0)}$	100	110	220	250	530	550	3000
	γ_c	0.03	0.03	$\sim$0.001	$\sim$0.001	$\sim$0.01	$\sim$0.01	0.02
	γ_y	0.32	0.25	0.18	0.14	0.11	0.11	0.08
	τ_c/Pa[b]	3.0	3.3	3.1	3.3	11.1	13.2	
	τ_y/Pa[c]	5.1	4.5	4.6	4.7	9.7	7.3	32
	G'_y/Pa	16	18	12	18	49	38	400
	$G'_{1\text{Hz},\ \gamma=0.05}$	88	95	133	139	406	380	3000 (γ = 0.001)
Frequency sweep	$G'_{1\text{Hz}}$/Pa	180	167	342	379	399	401	830 (γ = 0.001)
Creep	$G_{e(\text{peak})}$/Pa	51	—	61	—	—	—	7400
	$\eta_{(\tau\to 0)}$/Pa s	1.1 $\times$ 10^5	—	4.0 $\times$ 10^4	—	—	—	1 $\times$ 10^6
	$\tau_{y(\text{cr})}$/Pa	8.5	—	$>$10	—	—	—	71
Flow curves controlled shear stress–shear rate	$\eta_{(\tau\to 0)}$/Pa s	75 000	29 000	260 000	105 000	500 000	400 000	5e5–1E6
	$\tau_{y(\text{up})}$/Pa	19	13	22	22	59	59	75
	$\tau_{y(\text{down})}$/Pa	11	10	14	14	41	41	45
	γ_y		1.24		0.67		0.23	0.075

[a] Measurements performed on Bohlin CVO with a different hectorite sample prepared by the same protocols. [b] τ_c is the critical yield stress at the initial critical failure strain γ_c, evaluated as $G'_{\gamma\to 0}\gamma_c$. [c] τ_y is the effective yield stress at the strain γ_y where the G' and G'' curves cross, evaluated as $G'_y\gamma_y$. [d] BG = broken gel pre-conditioning protocol (see Rheological measurements), EG = equilibrium gel conditioning protocol.

falls dramatically at $\gamma_y \sim 0.1$, which is where G'' peaks and G' and G'' cross, quite sharply in this case. The pre-treatment protocol again shows little effect on the breakdown of the gel phase.

Turning to the frequency dependence of the complex shear moduli in the linear regime as shown in Fig. 1b, G' is again relatively independent of frequency, the upturn at low frequencies simply reflecting the growing gelation times at $\gamma < \gamma_y$ experienced by the fluids measured at low frequencies. G'' is similar to the other mixture in its frequency dependence but slightly lower in magnitude. At a strain of 0.05 the hectorite–gibbsite mixture is already well out of the linear regime, and $G' \sim 400$–500 Pa is consistent with the data in the strain sweep.

The kinetics of the structuring of the mixture as tracked by the build-up of G' over time are also shown in Fig. 2. Though the data for the hectorite–gibbsite mixture are much noisier than for the other fluids, it appears that there is a slight induction period after which G' rises more rapidly than for the other fluids to a higher limiting value.

The controlled stress continuous shear data (Fig. 6a) confirm the enhanced rheological properties of this fluid. The flow curve is displaced even further upwards from the pure hectorite suspension. The low shear viscosity is $\sim 5 \times 10^5$ Pa s and the gel yields sharply at 60 Pa (Fig. 6b). It shows the same shear thickening at low stresses, the abrupt jump from the low shear–high viscosity branch to the high shear–low viscosity branch to a shear rate of 30 s^{-1}, and on the down ramp follows to the high shear–low viscosity branch until a stress of ~ 50 Pa is reached and at a shear rate of ~ 3 s^{-1} rejoins the low shear branch with a stress of ~ 15 Pa.

Table 2 summarises the rheological parameters for the hectorite–gibbsite mixture. The addition of 0.25 wt% of gibbsite platelets has increased the plateau modulus of the hectorite gel from 100 Pa to 550 Pa, increased its effective yield stress by a factor of 6 to 60 Pa and enhanced the pre-yield effective viscosity by a factor of 5 to 5×10^5 Pa s. The synergy between the lath-like hectorite and the plate-like gibbsite is even more pronounced than with the rod-like boehmite.

Hectorite–Ludox CL

To complete the series of varying particle shape of the second component, we now consider a mixture of laths and spheres. Ludox CL is a cationic alumina-coated silica with a diameter of 12 nm, which is of the same order of magnitude as the diameter of the boehmite rods and the thickness of the gibbsite plates. These measurements were performed on a different batch of hectorite, so the concentrations are slightly different to those previously reported. This causes only minor differences in the magnitude of the results.

Fig. 7 shows the storage and loss moduli as a function of (a) applied strain at 1 Hz and (b) frequency at $\gamma = 0.001$ for the hectorite–Ludox CL mixture compared to pure hectorite at a base concentration of 2.8 wt%. Comparing this hectorite sample with the previous samples shown in Fig. 1, we see similar shaped curves, albeit with slightly different absolute values. As with the previous mixtures we see that addition of the cationic spheres has increased the storage modulus substantially, in this case from ~ 100 to over 1000 Pa, and reduced the critical strains to yield. γ_c falls from 0.03 to 0.02 and γ_y, where the G' and G'' curves cross, from ~ 0.35 to 0.08.

Creep measurements were then carried out on the hectorite–Ludox CL mixture. The creep curves are qualitatively similar to those for the boehmite–hectorite mixture shown in Fig. 3, especially at the lowest applied stresses. The data were fitted to the generalised Kelvin model and again excellent fits were obtained. The Kelvin parameters are given as a function of stress in the ESI† and depicted in Fig. 8. Fig. 8a clearly shows an effective yield stress of 71 Pa, where the creep viscosity drops dramatically from 1×10^6 to ~ 1 Pa s. Fig. 8b shows retardation times of ~ 5 s and ~ 100 s. Unlike the previous mixtures and the pure hectorite there is no peak in the relaxation times, instead a slow reduction in λ_2 as the effective

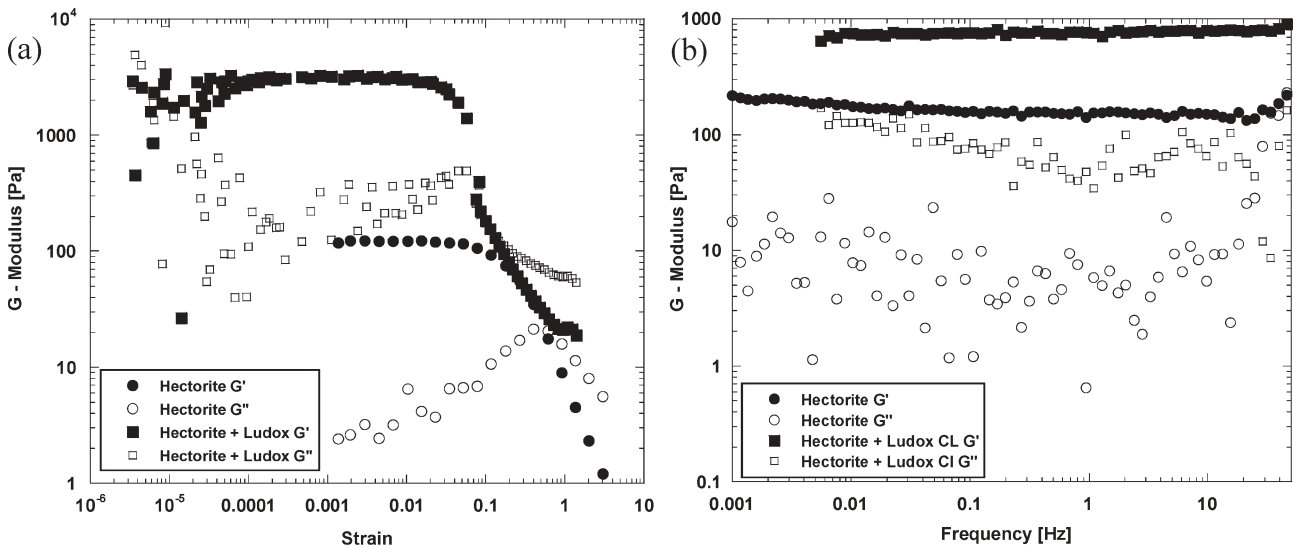

Fig. 7 Storage and loss moduli for 2.8% hectorite and 2.8% hectorite + 0.25% Ludox CL. (a) Strain dependence at 1 Hz. (b) Frequency dependence at $\gamma = 0.001$.

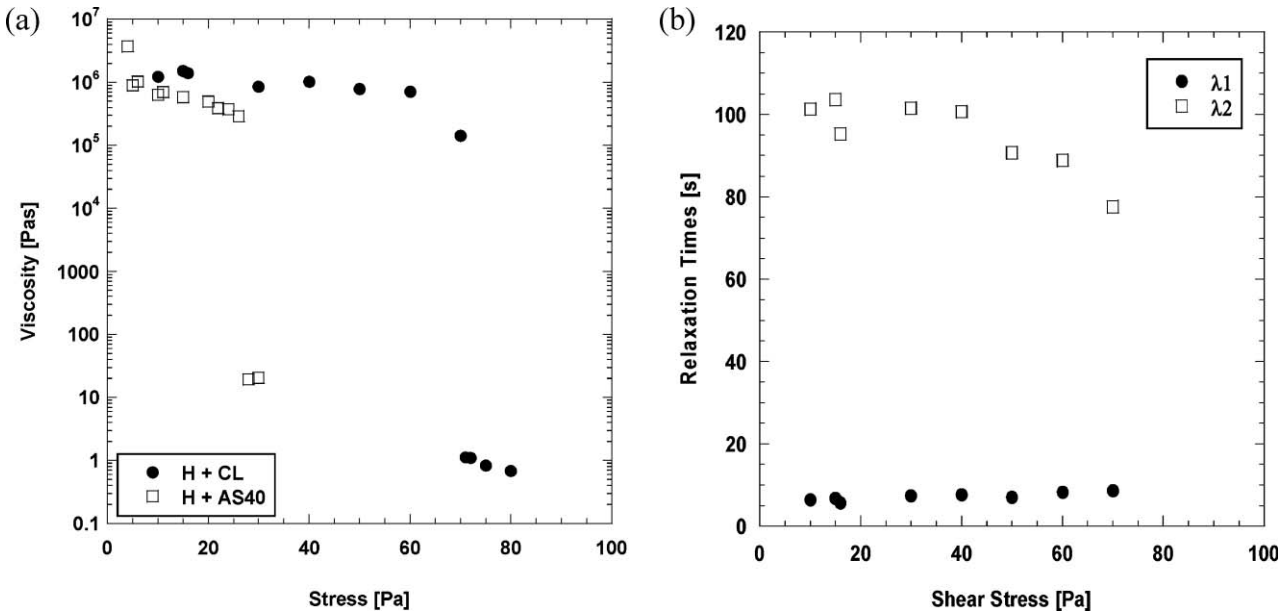

Fig. 8 Creep analysis for 2.8% hectorite + 0.25% Ludox silica. (a) Creep viscosity *versus* applied stress, closed symbols Ludox CL, open symbols Ludox AS40. (b) Relaxation times *versus* applied stress for 2.8% hectorite + 0.25% Ludox CL.

yield stress is approached. At the effective yield stress the retardation times must drop dramatically.

At high stresses, around the effective yield or transition stress, we see quite different behaviour. At $\leqslant$70 Pa we observe classic creep where the long-time low shear rate slope persists for at least 600 s. At 71 Pa and above, we observe a transition of the long-time slope to much higher values, but unlike for pure hectorite and the other mixtures, this transition is delayed in time. This delay time is strongly stress dependent – it decreases sharply with increasing stress. This is seen in Fig. 9 where at 75 Pa we see a sharp transition in the creep curve at t_c = 30 s. Below this time the strain rate is $\sim$1 s^{-1}, already a factor of 10^4 greater than at 70 Pa; above 30 seconds the fluid 'yields' rapidly to give a creep curve slope of $\sim$93 s^{-1}. As we increase the stress further, the initial slope remains essentially the same ($\sim$1 s^{-1}) whereas the transition time moves to increasingly earlier times. At 80 Pa for instance, t_c = 15 s. This behaviour is similar to that seen by Gopalakrishnan and Zukoski[27] on a thermoreversible gel system consisting of organophilic silica spheres in decalin.

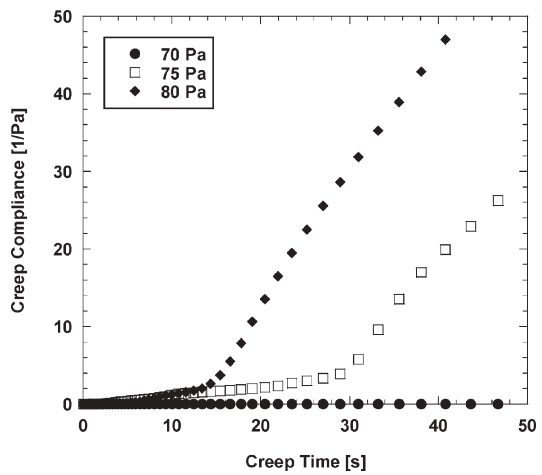

Fig. 9 Early-time data from 600 s duration creep experiments on the 2.8% hectorite + 0.25% Ludox CL suspension at applied stresses around the effective yield stress of 71 Pa (see Fig. 8).

The enhanced rheology is reflected in the controlled stress continuous shear data, Fig. 10a, where the curves for the hectorite–Ludox mixture are again displaced upwards and to the left of the hectorite data. As with the other mixtures, we find that the key features of the hectorite rheology are maintained, with the characteristic shear thickening at very low shear stresses–shear rates, a dramatic break in the curve when the sample yields at 20 Pa for the hectorite and 74 Pa for the mixture. The curve jumps several orders of magnitude in shear rate as the sample yields and shear thins, eventually joining the high shear branch at 100 s^{-1}. Unlike the other samples the hectorite–Ludox mixture shows a transition between high and low shear rate around 5 s^{-1} in both the up curve and down curve, slightly higher than the transition for the base clay suspension. We argue that this transition between the two branches of the flow curve near the transition stress is related to the delayed transitions observed in Fig. 9 between the early time and long time slopes of the creep curves. In fact each point in Fig. 10a is obtained by essentially carrying out a local creep measurement at increasing values of the applied stress and determining the resulting shear rate by averaging the strain change over the chosen measurement time window. As the transition elbow in Fig. 9 moves backwards towards lower times with increasing stress, and hence moves through this measurement time window, we expect the measured strain rate in the continuous shear experiment of Fig. 10a to move from the initial low stress value of $\sim 10^{-4}$ s^{-1} through the essentially constant time-slope value in Fig. 9 of 1 s^{-1} to the much higher values of the steeper long-time slopes, which increase with applied shear stress, as reflected in the right hand branch of Fig. 10a.

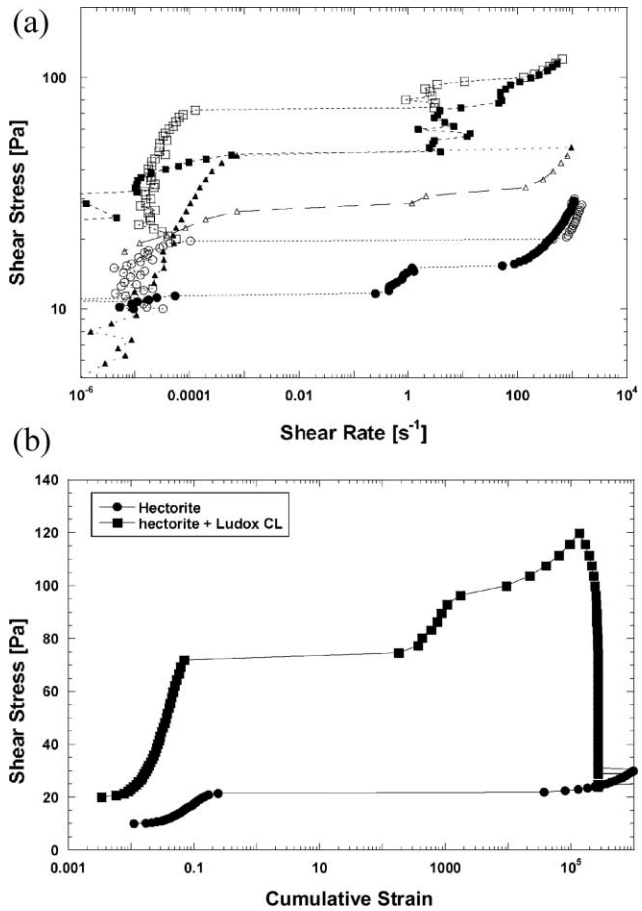

Fig. 10 a Controlled stress continuous shear rheology for 2.8% hectorite (circles), 2.8% hectorite + 0.25% Ludox Cl (squares), and 2.8% hectorite + 0.25% Ludox AS40 (triangles). Open symbols shear stress increasing, closed symbols shear stress decreasing. (b) Controlled stress continuous shear rheology for (circles) 2.8% hectorite and 2.8% hectorite + 0.25% Ludox Cl (squares). (a) Shear stress *vs.* shear rate. Open symbols shear stress increasing, closed shear stress decreasing. (b) Shear stress *vs.* cumulative strain.

Fig. 10b demonstrates the role of critical strain in the yielding phenomena quite conclusively. Here we plot the shear stress data as a function of the *accumulated strain* during the measurement. We calculate the accumulated strain from the shear rate multiplied by the total dwell time at each measurement point (54 s). Hectorite yields at γ_y = 0.25, and hectorite–Ludox CL at 0.08, in line with the oscillatory data.

Summarising the rheological data for the hectorite–Ludox CL mixture in Table 2, they show an entirely consistent picture from the three different techniques (oscillation, creep and continuous shear viscometry) of a gelled system with low-shear effective viscosity of 1×10^6 Pa s, an elastic modulus $\sim$3000 Pa, an effective yield stress of $\sim$70 Pa, and a yield strain of 0.08.

Hectorite–Ludox AS40

In order to discriminate between the effect of particle size/shape and charge, we carried out some measurements on a mixture in which the cationic Ludox CL was replaced by Ludox AS40, an anionic silica of identical particle diameter, 12 nm. For example, it can be seen in Fig. 10a that the hectorite-Ludox AS40 mixture also shows significant enhancement of the continuous controlled shear stress behaviour compared to hectorite, though not as marked as for the hectorite–Ludox CL mixture. The creep behaviour was similar for the two Ludox mixtures; Fig. 8a for the creep viscosity shows that the low stress creep viscosity for hectorite–Ludox AS40 is only slightly less than for hectorite–Ludox CL, whereas the creep yield stress is 25 Pa, five times the value for pure hectorite but considerably lower than the 71 Pa of hectorite–Ludox CL. Unlike the hectorite–Ludox CL mixture, however, the anionic silica blend retains a yield strain similar to pure hectorite dispersions. Overall the rheological behaviour of the two hectorite–Ludox mixtures were qualitatively similar in all flow modes, with the anionic AS40 system showing significant enhancements compares to hectorite, greater than for gibbsite and boehmite but less than for the cationic CL spheres.

The extremely high creep viscosity observed for this and many of the other systems is deserving of comment. The reproducibility of these measurements, and their consistency with the low-stress viscosities obtained in the continuous controlled shear experiments, indicate that these values are physically meaningful. Values in the range 10^5–10^6 Pa s have been observed recently for another colloid.[28] The ability with current generation rheometers to detect such high viscosities, corresponding to extremely low but finite shear deformations in response to low applied stresses, is causing a re-evaluation of the understanding of yield phenomena in complex fluids and soft solids.[29] 'Yield' is increasingly being seen not as the simple onset of flow but as a dramatic cooperative-like reduction in effective viscosity from an extremely high but finite value at low stresses to a much lower value that permits measurable flow, once a critical strain or stress has been exceeded resulting in major microstructural rearrangement.

Discussion

We have presented results on rheology enhancement in colloidal mixtures, a concept which has been exploited commercially in the area of clay-based drilling fluids where the use of mixed-metal hydroxides as viscosity extenders for montmorillonite clay dispersions was first suggested some 20 years ago by Burba and co-workers[2–4] This paper, which we believe to be the first comprehensive study of such effects on well-characterised model systems, is a sequel to Part I[1] where we investigated the rheology of the pure component mineral colloids. We focused particularly on the role of particle shape and how laths (hectorite) and platelets (gibbsite) differ from rods (boehmite) under similar conditions. Their rheological behaviour was found to be extremely rich and complex, differing significantly from the common monotonically increasing stress–strain flow curve often reported for clay-based dispersions. Despite the wide variation in gel intensity, a unifying picture of their rheology emerged; these viscoplastic materials displayed distinct and relatively simple behaviour at the extremes of deformation. At extremely low strains they behave as elasticoviscous solids with a very high viscosity, and at very large strain–strain rates as shear-thinning, weakly

elastic, low viscosity liquids. The transition region between the two extremes is very complex and is a function of its stress–strain-time history. By employing a multi-technique approach we were able to probe the transition behaviour in some detail. There is no unique 'yield stress' and a number of parameters are required to describe this *yield space*. It was observed that strain appeared to be the controlling factor governing disruption of the gel, the initial critical strains (where the gel structure begins to break down at the limit of the linear viscoelastic regime) being very small and in the order boehmite ($\sim$0.4) > hectorite ($\sim$0.3) > gibbsite ($\sim$0.1). This is the same order as the parameter α, the ratio of the hydrodynamic volume of the particles to their real volume (see Table 1), which increases from platelets to laths to rods. This was also reflected in the order of c^*, the critical overlap concentration at which on average the particles start to overlap and the repulsive double layers have a major effect: boehmite < hectorite < gibbsite.

By adding a second component we enrich the behaviour still further. Here we find that, although the mixtures follow the same general behaviour (elastoplastic solid–shear-thinning liquid with a complex yield space), addition of small amounts (<10% by weight of total solids) of the aluminasol minor component significantly enhances both the elastic and viscous characteristics of a base 2.5 wt% hectorite clay suspension initially at c/c^* $\sim$1.7. This dramatic enhancement and its dependence on particle shape is the unifying theme of this work. Specifically we find that all the rheological parameters increase in the order hectorite < or $\sim$ hectorite–boehmite < hectorite–gibbsite < hectorite–Ludox CL. For the oscillatory shear measurements, $G'_{(\gamma\rightarrow 0)}$ increases in the approximate ratio 1 : 2 : 5 : 30, τ_y in the ratio 1 : 1 : 2 : 6, G'_y in the ratio 1 : 1 : 2 : 20, $G'_{1\mathrm{Hz},\ \gamma=0.05}$ in the ratio 1 : 1.4 : 4 : 20. From the creep experiments $G_{e(peak)}$ increased most dramatically in the ratio 1 : 1: - : 1500, $\eta_{(\tau\rightarrow 0)}$ in the ratio 1 : 0.4 : - : 14 and $\tau_{y(cr)}$ in the ratio 1 : >1.2 : - : 8. Finally from the controlled stress continuous measurements $\eta_{(\tau\rightarrow 0)}$ increased in the ratio 1 : 3 : 10 : 20, $\tau_{y(up)}$ in the ratio 1 : 1.5 : 4.5 : 6, and $\tau_{y(down)}$ 1 : 1.5 : 4 : 4.5. The effects are both significant and consistent. In contrast to the storage shear modulus, effective viscosity and effective yield stress, the yield strains decrease in the order hectorite > hectorite–boehmite > hectorite–gibbsite > hectorite–Ludox CL. From the oscillatory measurements γ_y decreases in the ratio 1 : 0.6 : 0.3 : 0.25 whereas from the controlled stress continuous shear it decreases in the ratio 1 : 0.5 : 0.2 : 0.06, again demonstrating a consistent trend. In other words the stronger gels are also the most fragile, and reflect to a large extent the strain sensitivity of the minor component.[14] Where the hectorite–Ludox AS40 mixture has been investigated, its rheological parameters lie in between hectorite–Ludox CL and hectorite–gibbsite.

So far we have just made an inventory, which is rich and varied. These interesting findings invite the question as to their physical origins. In general terms it is likely that underpinning the observed behaviour is the extent to which adding particles of different size and shape to a hectorite gel will, on the one hand, disrupt the structure of the original gel and hence induce local packing changes, which for similarly charged particles might be expected to weaken the gel, and on the other hand enhance structuring to some extent by introducing oppositely charged particles between which there will be attractive coulombic interactions, which might be expected to strengthen the gel. The overall effect will be a balance between these (and maybe other) effects, which in turn will be influenced by the dimensions of the added particles (how well they 'fit' between the hectorite platelets), their charge (density and spatial distribution) and their shape, which will influence both the packing and the charge distribution.

Under the pH and low-salinity conditions of the experiments hectorite has a high negative (face) surface charge, (though the preparation procedure may have given rise to some release of magnesium ions, which could give particle edges some cationic character), and the minor component is positively charged. The base hectorite suspension forms a repulsive gel, whereby the overlap of the electrical double layers generates repulsive forces between the particles causing a cooperative resistance to motion and an elastic response to small applied stresses. Adding the second (oppositely charged) particles gives rise to a heteroflocculation interaction, which appears to strengthen the gel. Work with MMH–clay dispersions[3,14] shows that the maximum rheology enhancement typically occurs at a mass ratio of the clay to the second colloid in the range of 8 : 1 to 12 : 1, which corresponds to charge neutrality. One may therefore postulate that, under conditions where the hectorite is already hydrodynamically close-packed ($c > c^*$, where c^* is based on the hydrodynamic volume as defined in Table 1), the minor component enhances clustering and spatial percolation by bridging the hectorite particles due to attractive coulombic interactions, reinforcing the gel electrostatically and mechanically. Increasing the concentration of the second component up to the charge-neutrality point will increase bridging interactions and hence the gel strength. Keren[30] and Neaman and Singer[31] found similar effects with mixed kaolinite–montmorillonite, and mixed montmorillonite–palygorskite suspensions, respectively, where again a ratio of 10 : 1 appeared to be optimum.

The efficacy of the second colloid in enhancing the hectorite gel will depend on its charge density, increasing the inter-particle forces, the extent to which it can fit into the existing particle network without disrupting the gel structure and on the number of added particles, which will influence the number of potential bridging interactions. As the essential rheological character of the hectorite gel persists, this suggests that the structure of the dispersion has not been significantly disrupted by the addition of the second component. In our mixtures we observe a trend of enhanced gel strength from rods to plates to spheres, in reverse order to their hydrodynamic volumes, which implies that particle packing is a significant factor, the spheres perhaps fitting more easily into the clay gel with less disruption of the structure than do the rods or plates. Since the same mass of minor component is added in all cases, the number of added silica particles is significantly greater than for the gibbsite platelets and the boehmite rods, enhancing the potential for gel reinforcement through bridging interactions. The size of the silica spheres may also be a contributing factor, being comparable to the minimum dimension of the host lath particles. It would be interesting to confirm this by experiments with spheres of different sizes; the recent work of Baird

and Walz[22] with Ludox silica–kaolinite mixtures shows yield stresses dependent on the Ludox particle size, with the strongest gels occurring with the smallest spheres. The picture of the second component fitting into and mediating the existing gel structure fits with the strain sensitivity of the mixtures reflecting the 'yield strain' response of the pure minor component.

We can attempt to quantify these effects to some extent. The larger the number of secondary particles, the greater the number of potential bridges or 'cross-links', and hence the enhancement of rheological parameters such as low-shear gel viscosity and modulus. Since the same mass of secondary component is added, the ratio of the number of particles added for spheres, platelets and rods is approximately 280 : 1 : 2. The major reinforcement by the silica spheres is therefore understandable on this basis, but the greater effectiveness of gibbsite platelets compared to the boehmite rods suggests that additional factors come into play. As a measure of the ability of the minor component to pack around the hectorite laths, we can define a packing ratio as: hectorite surface area/additive hydrodynamic cross-section $\sim 2(L_1L_2 + L_1d + L_2d)$ (hectorite)/L_1^2(additive). This quantity decreases as we move from Ludox spheres (200) through gibbsite platelets (4.5) to boehmite rods (0.8). This indicates that the potential coordination number of a hectorite lath for clustering and gel formation also increases in line with the order of rheological enhancement. Given the central role of the minor component in determining the gel properties, through the postulated particle-bridging mechanism, it is not unreasonable to expect that the strain sensitivity of these properties is related to the maximum dimension of the bridging particles. On this basis the yield strain should decrease in the order of L_1 *viz* boehmite > gibbsite > Ludox CL, as indeed is observed. These arguments are clearly crude, but in the absence of a more detailed understanding of the particle interactions and resulting microstructure, they probably encapsulate the essential physics.

In addition, we can begin to disentangle the relative contribution of geometric and coulombic interactions by replacing the cationic particles by anionic ones of like shape. We have done this for one of our mixed dispersions using Ludox AS40, 12 nm anionic silica spheres, in place of Ludox CL. Fig. 8a and Fig. 10a show the comparison between the two Ludox–hectorite mixtures in creep experiments and controlled-stress continuous shear flow. The anionic silica spheres also enhance the gel, but not as much as for the cationic silica. τ_y increases from 20 Pa for pure hectorite to $\sim$30 Pa with the anionic silica and to 71 Pa with the cationic silica. G_e also increases from $\sim$100 Pa to $\sim$250 Pa and then to >3000 Pa. While it is possible that the anionic silica spheres are interacting with some cationic clay lath edge sites in a similar but less effective heteroflocculation, we believe that with Ludox AS40 we are seeing an enhancement of the repulsive gel brought about through additional particle crowding; the strain sensitivity of the gel appears not to be significantly reduced compared to pure hectorite as it is with the cationic spheres, arguing against bridging flocculation. Here therefore the main driver for gel formation is electrostatic repulsions, as it is for the pure components. In replacing 10 wt% of the hectorite (α = 160, see Table 1) by AS40 silica, for which (α = 1) the hydrodynamic volume is the same as the actual particle volume, the free volume of the dispersion and the mean particle separation are significantly reduced. Hence due to enhanced particle packing, the viscosity, shear modulus *etc.* all increase, although not as much as for the attractive gel. Based on the trends observed with the cationic particles, we might expect that anionic plates or rods would pack less effectively with the clay laths and the effect could be weaker, or even lead to a reduction in the gel strength. It would be instructive to investigate the rheology of a natural hectorite–laponite mixture in this context.

Clearly these hypotheses require detailed evaluation by further investigations of the microstructure of these dispersions and how this changes in relation to the rheological properties as the system deforms under applied stresses. The above concepts are similar to those put forward by Shalkevich *et al.*[32] for dynamical arrest and cluster formation in pure clay dispersions following neutron, X-ray and light scattering studies. Their model for cluster and gel formation could be extended to include particle mixtures and heteroaggregation phenomena, in line with the above arguments. A range of other models have been proposed to describe qualitatively and quantitatively these gelation phenomena in concentrated dispersions of spherical particles. These include mode-coupling theories,[33–35] cage models[36,37] and models based on shear-mediated building and disruption of fluid microstructure.[38–41] However at this stage it is not clear that any of these can be applied directly to the systems and data presented here and future progress certainly needs to be informed by further experimental investigation of our systems on a range of length and time scales, to complement the bulk rheological observations.

So at this stage no definitive conclusion can be drawn or detailed model be constructed to explain fully the results of this work. In order to give greater insight into the microstructure of the mixed suspensions and the flow-induced changes as the dispersions undergo this complex transition from an elasto-viscous gel to a viscoelastic liquid, it would be useful to study how these changes influence the local microscopic (maybe inhomogeneous) flows within a rheometer through flow imaging. Ideally one would measure microstructural changes, local flow velocity and stress distributions and bulk rheological parameters simultaneously on the same systems. The combination of flow patterns and microstructure has been successfully measured in the case of dense suspensions of spherical particles through confocal microscopy using fluorescently labelled particles.[42,43] It would be interesting to extend such measurements to the anisotropic particles used here. New microrheology measurements[44] using videoparticle tracking offer a tantalising glimpse of the behaviour of very low concentration hectorite suspensions, showing the development of a gel with significant spatial anisotropy.

Although the physical origins of the phenomena observed in this work have yet to be fully established, the results presented here on well-characterised model systems provide a baseline study for future exploitation and understanding of the rheology and dynamics of mixed colloidal dispersions. In particular, they suggest that major enhancements in the strength of gels and the viscosity of concentrated suspensions,

as well as the kinetics of their transition between the gelled and liquid-like states, can be achieved by adding low concentrations of oppositely charged colloids to single-component mineral dispersions. It seems that spherical particles of size comparable to the minimum dimension of the main component may be particularly effective in this regard, although experiments with spheres of different sizes would have to be done to confirm that it is this diameter that is most effective, as in recent studies on kaolinite–silica systems.[22] This study confirms and extends the earlier observations on clay–MMH and clay–aluminasol mixed dispersions and suggests that rheological enhancement and control of the rates of sol–gel transitions for product applications can be achieved using relatively low cost commercially available colloidal particles, such as Ludox CL and related systems.

Acknowledgements

Annemieke J. T. ten Brinke was financially supported by the Nederlandse Organisatie voor Wetenschappelijk Onderzoek (NWO) and by Schlumberger Cambridge Research. The authors also acknowledge financial support from the SoftComp EU 6th Framework Network of Excellence, which enabled them to carry out exchange working visits as part of this research. They thank Edo Boek for helpful discussions.

References

1 A. J. W. ten Brinke, L. Bailey, H. N. W. Lekkerkerker and G. C. Maitland, *Soft Matter*, 2007, **3**, 1145–1162.
2 J. L. Burba, III and A. L. Barnes, US 4 664 843, 1987.
3 J. L. Burba, W. F. Tehan, F. D. Hamilton, W. E. Holman, C. Porzucek, C. P. Christenson and J. McKenzie, ''Field evaluations confirm superior benefits of MMLHC fluid system on hole cleaning, borehole stability, and rate of penetration.'', Proceedings of IADC/SPE 1990 Drilling Conference, Society of Petroleum Engineers of AIME, SPE, Dallas, TX, USA, 1990, pp. 371–380.
4 C. R. Crabb, J. L. Burba, III and W. E. Holman''New inorganic attapulgite extender provides stable rheology and supports heavy cuttings even under severe conditions.'' Proceedings of 1989 SPE International Symposium on Oilfield Chemistry. Society of Petroleum Engineers of AIME, SPE, Houston, TX, USA, 1989, pp. 219–226.
5 A. Wierenga, A. P. Philipse, H. N. W. Lekkerkerker and D. V. Boger, *Langmuir*, 1998, **14**, 55–65.
6 A. M. Wierenga and A. P. Philipse, *Colloids Surf., A: Physicochem. Eng. Asp.*, 1998, **137**, 355–372.
7 A. M. Wierenga, T. A. J. Lenstra and A. P. Philipse, *Colloids Surf., A: Physicochem. Eng. Asp.*, 1998, **134**, 359–371.
8 S. M. Jogun and C. F. Zukoski, *J. Rheol.*, 1999, **43**, 847–871.
9 D. Bonn, P. Coussot, H. T. Huynh, F. Bertrand and G. Debrègeas, *Europhys. Lett.*, 2002, **59**, 786–792.
10 P. Coussot, Q. D. Nguyen, H. T. Huynh and D. Bonn, *J. Rheol.*, 2002, **46**, 573–589.
11 P. B. Laxton and J. C. Berg, *J. Colloid Interface Sci.*, 2006, **296**, 749–755.
12 L. Onsager, *Annu. Rev. Phys. Chem.*, 1949, **51**, 627–659.
13 M. C. D. Mourad, J. E. G. J. Wijnhoven, D. D. Van't Zand, D. Van Der Beek and H. N. W. Lekkerkerker, *Philos. Trans. Math. Phys. Eng. Sci., Ser.A*, 2006, **364**, 2807–2816.
14 G. Lagaly, O. Mecking and D. Penner, *Colloid Polym. Sci.*, 2001, **279**, 1097–1103.
15 P. Lange, G. Keilhofer and J. Plank, US 6 475 959, 2002.
16 F. Van Der Kooij, H. N. L. Lekkerkerker and E. S. Boek, EP 1 414 926, 2004.
17 F. M. Van Der Kooij and H. N. W. Lekkerkerker, *Langmuir*, 2000, **16**, 10144–10149.
18 S. M. Oversteegen and H. N. Lekkerkerker, *J. Chem. Phys.*, 2004, **120**, 2470–2474.
19 S. M. Oversteegen, J. G. E. J. Wijnhoven, C. Vonk and H. N. W. Lekkerkerker, *J. Phys. Chem. B*, 2004, **108**, 18158–18163.
20 S. K. Rhodes and J. A. Lewis, *J. Am. Ceram. Soc.*, 2006, **89**, 1840–1846.
21 A. A. Louis, E. Allahyarov, H. Löwen and R. Roth, *Phys. Rev. E: Stat., Nonlinear, Soft Matter Phys.*, 2002, 65.
22 J. C. Baird and J. Y. Walz, *J. Colloid Interface Sci.*, 2007, **306**, 411–420.
23 J. C. Baird and J. Y. Walz, *J. Colloid Interface Sci.*, 2006, **297**, 161–169.
24 M. P. B. Van Bruggen, *Langmuir*, 1998, **14**, 2245–2255.
25 H. A. Barnes, *J. Non-Newtonian Fluid Mech.*, 1997, **70**, 1–33.
26 J. W. Goodwin and R. W Hughes, *Rheology for Chemists*, Royal Society of Chemistry, Cambridge, 2000.
27 V. Gopalakrishnan and C. F. Zukoski, *J. Rheol.*, 2007, **51**, 623–644.
28 G. P. Citerne, P. J. Carreau and M. Moan, *Rheol. Acta*, 2001, **40**, 86–96.
29 H. A. Barnes, *Appl. Rheol.*, 2007, **17**, 43110-1–43110-5.
30 R. Keren, *Soil Sci. Soc. Am. J.*, 1989, **53**, 725–730.
31 A. Neaman and A. Singer, *Clays Clay Miner.*, 2000, **48**, 713–715.
32 A. Shalkevich, A. Stradner, S. K. Bhat, F. Mulle and P. Schurtenberger, *Langmuir*, 2007, **23**, 3570–3580.
33 J. Bergenholtz and M. Fuchs, *Phys. Rev. E: Stat. Phys., Plasmas, Fluids, Relat. Interdiscip. Top.*, 1999, **59**, 5706–5715.
34 L. Fabbian, W. Götze, F. Sciortino, P. Tartaglia and F. Thiery, *Phys. Rev. E: Stat. Phys., Plasmas, Fluids, Relat. Interdiscip. Top.*, 1999, 59.
35 K. S. Schweizer and E. J. Saltzman, *J. Chem. Phys.*, 2003, **119**, 1181–1196.
36 M. Mezard and G. Parisi, *J. Chem. Phys.*, 1999, **111**, 1076–1095.
37 K. N. Pham, S. U. Egelhaaf, P. N. Pusey and W. C. K. Poon, *Phys. Rev. E: Stat., Nonlinear, Soft Matter Phys.*, 2004, **69**, 115031–1150313.
38 D. C. H. Cheng and F. Evans, *J. Appl. Phys.*, 1965, **16**, 1599–1617.
39 F. Moore, *Br. Ceram. Soc. Trans.*, 1959, **58**, 470–484.
40 P. C. F. Møller, J. Mewis and D. Bonn, *Soft Matter*, 2006, **2**, 274–283.
41 N. A. Spenley, M. E. Cates and T. C. B. McLeish, *Phys. Rev. Lett.*, 1993, **71**, 939–942.
42 L. Isa, R. Besseling, E. R. Weeks and W. C. K. Poon, *J. Phys. Conf. Ser.*, 2006, **40**, 124–132.
43 D. Derks, H. Wisman, A. Van Blaaderen and A. Imhof, *J. Phys.: Condens. Matter*, 2004, **16**, S3917–S3927.
44 P. Cicuta and A. M. Donald, *Soft Matter*, 2007, **3**, 1449–1455.

